Predictive control algorithms for congestion management in electric power distribution grids

Ioannis Kalogeropoulos, Haralambos Sarimveis*

School of Chemical Engineering, National Technical University of Athens, Heroon Polytechneiou 9, Zografou, Athens, Greece

ARTICLE INFO

ABSTRACT

In this paper, model predictive control methodologies are developed to address two main issues which arise in electric power distribution systems, namely the congestion of the distribution lines and the balancing problem. Consumer energy demand is divided into an uncontrollable part, a controllable part that can be either stored in energy storage devices in order to be consumed at later times or shifted in time in the form of hourly consumption or a consumption that maintains a pattern. Demand – response strategies involve consumers actively in the balancing effort and are part of the MPC methodologies, which are formulated as Mixed Integer Quadratic Program optimization problems involving both continuous and binary variables. Finally, these new developments are tested on the IEEE European Low Voltage Test Feeder which highlights the performance of the proposed control schemes.

© 2019 Elsevier Inc. All rights reserved.

1. Introduction

Model predictive control (MPC) is a popular control method that has been used extensively in the energy sector. This method owes its popularity to its ability to handle multivariate processes and address state and input constraints explicitly [1]. According to this method, current and future manipulated inputs are optimized based on the current state of the system and the future predictions provided by a dynamic linear or nonlinear model of the system. The standard MPC problem formulation minimizes a quadratic cost function, which penalizes both the control energy and the deviations of the process state from their set-points [2].

In classic Automated Generation Control (AGC), units that provide the base load (e.g. fossil fuel-fired power plants) should be in reserve for a possible shortage of energy to the grid [3]. This balancing problem is traditionally solved by a centrally located entity, the so called Balance Responsible Entity (BRE), by activating or deactivating controlled reserves. This balancing problem is traditionally solved by a centrally located entity, the so called Balance Responsible Entity (BRE), by activating or deactivating controlled reserves. This fully centralized control approach is limited by the large scale power networks that spread over large geographic areas. On the other hand, the decentralized control philosophy leads into poor performance, as it neglects interactions among the subsystems. To overcome these barriers, distributed control has been introduced. According to this philosophy, a number of controllers dedicated to different subsystems carry out their calculations locally, yet they communicate in achieving the closed loop process objectives [4].

---

* Corresponding author.
E-mail address: hsarimv@central.ntua.gr (H. Sarimveis).

Nomenclature

AGC	Automated Generation Control
BRE	Balance Responsible Entity
BRP	Balance Responsible Party
CMPC	Centralized Model Predictive Control
CPP	Critical peak Pricing
DAM	Day Ahead Market
DMPC	Distributed Model Predictive Control
DR	Demand Response
DSO	Distribution System Operator
ESS	Energy Storage Systems
HP	Hourly Pricing
HVAC	Heating Ventilation and Air Conditioning
μCHP	micro Combined Heat and Energy Power
MPC	Model Predictive Control
PV	Photovoltaic energy system
RES	Renewable Energy Sources
TCL	Thermostatically Controlled Loads
LVTF	Low Voltage Test Feeder

Indexes

k	current time instant
i	specific BRP
l	time instant within the control horizon
c	specific consumer under BRP i
j	specific distribution line

Parameters

n_L	number of distribution lines
n_B	number of BRPs
n_D	number of nodes
m_i	number of consumers under BRP i
N_p	prediction horizon
N_c	control horizon

Constraints

p_i^{min}	lower limit of $\acute{p}_i$
p_i^{max}	upper limit of $\acute{p}_i$
$p_{i,|A-B|}^{max}$	maximum allowable difference between phases A and B
$p_{i,|A-C|}^{max}$	maximum allowable difference between phases A and C
$P_{i,|B-C|}^{max}$	maximum allowable difference between phases B and C
f^{max}	vector of upper bounds on energy flows

Variables

p_i	total consumption
$\bar{p}_i$	controllable consumption
$\tilde{p}_i$	uncontrollable consumption
$\acute{p}_i$	consumption to/from the energy storage device
e_i	energy stored in the storage device
D_i	diagonal square matrix with the drain losses
t_i	partial energy flow caused by BRP i
R_i	matrix indicating the interconnections of BRP i
f	vector containing total energy flows through the distribution lines
$q_{bal,i}$	balancing energy
$q_{spot,i}$	energy bought at the DAM
$\bar{P}_i$	matrix of uncontrollable consumptions for the full control horizon
$\tilde{P}_i$	matrix of controllable consumptions for the full control horizon
$\hat{P}_i$	matrix of shiftable consumptions of hourly duration for the full control horizon

$\breve{P}_i$	matrix of shiftable consumption maintaining a pattern for the full control horizon
$B_{i,c}$	binary matrix for the hourly shiftable consumptions
$T_{d,c}$	time duration of shiftable consumption having a particular pattern
$\delta_{i,c,\,1}$	binary vector indicating the starting period of shiftable consumption having a particular pattern
$\delta_{i,c,\,j}$	binary vector indicating the time instants the shiftable consumption will be consumed
λ	Lagrange multipliers associated with the coupling constraints
Given consumptions	
$\hat{p}_i$	shiftable consumption of hourly duration
$\breve{p}_i$	shiftable consumption of a particular pattern

The combination of distributed control philosophy with the advantages of MPC results in the so called distributed MPC (DMPC), which is able to handle the control problem of large interconnected networks. Such a control approach has been used in [3] and [5] where the AGC problem was solved by incorporating the iterative exchange of information between the local subsystems. Also, in [6] distributed MPC is used to solve the balancing problem by actively controlling a portfolio of fossil fuel fired power plants to cope with the fluctuations from the renewable energy plants, such as wind farms. A limitation of these control strategies is that they involve only the production side of the distribution system. In a Smart Grid implementation both producers and consumers are equipped with control capabilities that allow them to participate in the balancing effort. The interaction between the power grid and consumers under power market regulations is known in the literature as demand response (DR). A comprehensive survey on demand response and smart grids has been presented in [7].

DR allows consumers to move or shift loads in time in order to meet the production side of the grid. In particular, thermostatically controlled loads (TCLs) in buildings such as air conditioners, refrigerators and water heaters are well-suited to load shifting in time by exploiting the large time constants of these devices as it is the case in [8]. In [9] the effects of DR on distribution system under two mechanisms of dynamic pricing, namely Critical Peak Pricing (CPP) tariff and Hourly Pricing (HP) were examined through numerical examples. In [10] a novel DR estimation framework for residential and commercial buildings was presented where the shifting loads were the heating ventilation and air conditioning (HVAC) system alongside additional TCLs. In [11] a predictive method to control power flows of Energy Storage Systems (ESS) and Photovoltaic (PV) was proposed. In [12] a procedure for optimal battery sizing of smart home using convex programming was presented. Plug-in electric vehicles may serve as DR consumption also. In [13] the coordinating charging of plug-in electric vehicles in a distributed control manner was proposed. The decomposition of the original problem was achieved via dual decomposition, where Lagrange multipliers were used in order for the dual function to be derived. Also, in [14] an optimal energy management strategy was developed for a smart home, where the coupling among plug-in electric vehicle, renewable and home battery was studied.

The penetration of renewable energy sources (RES) in smart grids and the general uncertainty of electricity demand as it is described in [15] and [16] have also led to overloads of the existing distribution network. Network constraints pose limitations on the amount of power that can be transferred between two nodes of the network, so that in practice it may not always be possible to fully meet conflicting interests. The consideration of these constraints on distribution grid is referred to as congestion management [17]. After the deregulation of the energy market [18], the markets have taken the responsibility for congestion management of the grid instead of regulations. The above mentioned DR strategies fail to take into consideration the conflicting interests among different Balance Responsible Parties (BRPs) or aggregators of the network as they assume that at every time instant the full state of the system is known, but this is very unlikely to happen in real conditions due to the competitive nature of the energy market.

An approach on this direction can be found in [19] and [20]. In [20],particularly, the existing situation in energy market is taken into account and is the starting point for the transition from the current situation of distribution grid to that of a smart grid. The energy market taken into consideration was that of the Day Ahead Market (DAM) [21], where the energy demand for the next 24 h is bought by BRPs in advance. However, due to uncertainties in RES generation and consumer energy demands, there are always differences between predicted energy demands and actual consumption. To deal with this problem, BRPs can trade the so-called balancing energy with the Distribution System Operator (DSO), who is responsible for maintaining the balance between production and consumption [22]. In that way, both successful congestion management and the economic viability of the system are achieved. BRPs can additionally exploit flexible consumption to minimize the difference between the energy they buy at the DAM and the energy which is actually consumed under their authority. The work of Biegel et al. [20] considers energy storage as an option for consumers to participate in balancing efforts and presents both centralized MPC and DMPC strategies for minimizing energy balancing costs of BRPs.

This paper extends the DAM structure presented in [20], by considering additional DR options for the consumers. In particular, we consider that part of the hourly energy load can be shifted in time. We also consider shifting of patterns that need multiple time periods to be completed. Consideration of these options introduces binary variables to the formulation of the MPC optimization problem, rendering our system a hybrid one, because of the simultaneously existence of continuous dynamics and discrete events. While there has been extensive work over the last years on analysis and control of hybrid
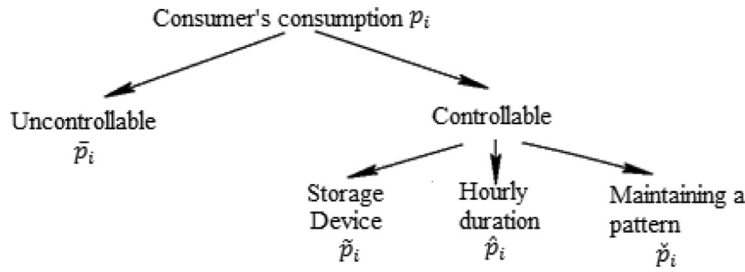
Fig. 1. Distribution of a customer energy consumption into uncontrollable consumption and three categories of controllable consumption.

systems, distributed MPC of hybrid systems is a research topic that has not received much attention [4]. In [23] and [24] distributed MPC for controlling micro Combined Heat and Energy Power (μCHP) in network and household level respectively were proposed. In [25] a distributed optimal control point of view applicable to a network of households with production devices, but also demand side control was proposed, however in neither of them the energy market or the congestion problem of the distribution lines of the grid were taken into account. In this direction, the main contribution of this paper is the presentation of an agent based DMPC control strategy incorporating binary decision variables to deal with both balancing and congestion management of distribution grid by taking into consideration the energy market aspect and DR techniques. The feasibility of the proposed algorithms as well as the its computational efficiency and scaling to real-life scenarios and the possible substitution of the centralized control scheme by the distributed one are tested on the IEEE European Low Voltage Test Feeder (IEEE ELVTF) [26], consisting of fifty five consumers, under three different scenarios. The proposed control scheme should be considered as an upper or intermediate control layer in a hierarchical control configuration, which computes the optimal steady state of the system under consideration.

The structure of the rest of the paper is as follows; In Section 2 a brief description of the model under consideration is given. Here, the reader is advised to refer to [20] for further information about the structure of the grid, the dynamics and the constraints which govern the system. In Section 3, two optimal DR strategies are developed and thoroughly described, alongside the centralized and distributed MPC algorithms which were used to deal with both congestion management and balancing problems. In Section 4, different case studies and scenarios are presented in order to illustrate the performance of the proposed MPC schemes. Finally, Section 5 contains the conclusions of this work.

2. Problem formulation

As mentioned in the introduction, the model described in [20] has been taken and properly adjusted in order to be used in the IEEE ELVTF. This section presents the notation and a brief description of the basic components of the system necessary for the rest of the paper and focuses on the model extension that take into account additional DR options.

We assume a radial topology distribution grid comprising of n_L distribution lines, n_B BRPs, n_D nodes and m_i consumers under the i th BRP. For the rest of the paper we use k to indicate the time instant and a sampling time of one (1) hour has been considered.

Consumers belonging to the *i*th BRP are characterized by hourly energy consumption (in kWh) which formulate a vector $p_i = (p_{i,1}, \ldots, p_{i,m_i}) \in \mathbb{R}^{m_i}$ consisting of two parts namely: the controllable part $\tilde{p}_i \in \mathbb{R}^{m_i}$ and the uncontrollable part $\bar{p}_i \in \mathbb{R}^{m_i}$. The former one can be further divided into a consumption corresponding to the energy flow to/from the storage device $\dot{p}_i \in \mathbb{R}^{m_i}$, a shiftable consumption of hourly duration denoted as $\hat{p}_i \in \mathbb{R}^{m_i}$ and a shiftable consumption which maintains a particular pattern denoted as $\breve{p}_i \in \mathbb{R}^{m_i}$. Fig. 1 presents graphically the distribution of consumers' consumption which used in this paper.

The total energy consumption of consumers under BRP-*i* at a given time period k is given by the summation of the uncontrollable consumption and the three categories of controllable consumption:

$$p_i(k) = \bar{p}_i(k) + \tilde{p}_i(k) \;\; = \;\; \bar{p}_i(k) + \dot{p}_i(k) + \hat{p}_i(k) + \breve{p}_i(k) \tag{1}$$

The energy flows to/from the storage devices are subject to hourly energy constraints:

$$p_i^{min} \leq \dot{p}_i(k) \leq p_i^{max} \tag{2}$$

where, p_i^{min} and $p_i^{max} \in \mathbb{R}^{m_i}$ are the lower and upper limits respectively on the energy transferred to/from the energy storage devise during an hour. According to this notation, $\dot{p}_i(k) < 0$ means that the storage device is releasing energy, while $\dot{p}_i(k) > 0$ means that the storage device is filling up with energy. Also, non-dispatchable producers can be included as negative consumers. The dynamics of the stored energy vector $e_i = (e_{i,1}, \ldots, e_{i,m_i}) \in \mathbb{R}^{m_i}$ are described by the following equation:

$$e_i(k + 1) = D_i e_i(k) + \dot{p}_i(k) \tag{3}$$

where, $D_i \in \mathbb{R}^{m_i \times m_i}$ is diagonal square matrix containing the proportional drain losses of each energy storage. The storage is subject to the following constraint:

$$0 \leq e_i(k) \leq e_i^{max} \tag{4}$$

Every BRP contributes to the loading of the distribution lines. The partial flow caused by the ith BRP to the n_L distribution lines is denoted as $t_i \in \mathbb{R}_+^{n_L}$. Accordingly, the relation that describes the partial flow caused by the BRP i is given by:

$$H_i * t_i(k) = R_i * p_i(k) \tag{5}$$

where, $R_i \in \mathbb{R}^{n_L \times m_i}$ is a matrix whose elements are given by:

$$(R_i)_{mn} = \begin{cases} 1, & \text{if consumer } m \text{ is suplied through link } n \\ 0, & \text{otherwise} \end{cases}$$

and $H_i \in \mathbb{R}^{n_D \times n_L}$ is a matrix whose elements are given by:

$$(H_i)_{mn} = \begin{cases} 1, & \text{if flow } n \text{ enters node } m \\ -1, & \text{if flow } n \text{ leaves node } m \\ 0, & \text{if flow } n \text{ is not connected to node} m \end{cases}$$

Finally, the total flows $f = (f_1, \ldots, f_{n_L}) \in \mathbb{R}_+^{n_L}$ are given by:

$$f(k) = \sum_{i=1}^{n_B} t_i(k) \tag{6}$$

where, f_j is the total energy flow through line j. The distribution line energy flows are subject to constraints:

$$f(k) \leq f^{max} \tag{7}$$

where, $f^{max} \in \mathbb{R}_+^{n_L}$ is the upper bound, defined by the upper hierarchically control layer in order to protect the distribution system from excessive energy consumption.

Each BRP buys energy through the DAM for each hour of the next day. This energy is denoted as q_{spot}. If this energy does not fit with the actual hourly consumption of the consumers the BRP must settle the difference with the DSO. The balancing energy of BRP i at each time period k is given by:

$$q_{bal,i}(k) = \mathbf{1}^T p_i(k) - q_{spot,i}(k) \tag{8}$$

where $\mathbf{1}$ is a column vector of all ones multiplying the column vector of dimension m_i containing the total power consumptions of all consumers belonging to BRP i. The balancing energy described by Eq. (8), is usually disadvantageous for the BRP due to the prices on trading balancing energy. This energy difference is paid by the BRP to the DSO one hour after it is consumed and needs to be minimized. The standard quadratic form of this energy difference that will be used in the MPC formulations can be written as follows:

$$h_i\big(q_{bal,i}(k)\big) = \big\| \mathbf{1}^T p_i(k) - q_{spot,i}(k) \big\|_2^2 \tag{9}$$

In this paper we present two model predictive control (MPC) approaches, namely centralized MPC (CMPC) and distributed MPC (DMPC), for optimally controlling the system by incorporating demand respond strategies. The MPC scheme is a widely used and popular control configuration for industrial and process applications, and owes its popularity to the inherent ability of the method to handle multivariate processes and to explicitly address state and input constraints [27]. The key concept of MPC is that at each discrete time instant k, an optimization problem is formulated and solved with respect to current and future manipulated variables over a control time horizon consisting of N_c time periods. The formulation of the optimization problem is based on the knowledge of the current state of the system and the prediction of its evolution over a finite prediction time horizon consisting of N_p time periods ($N_c \leq N_p$), through the existence and application of a dynamic discrete-time model of the system. Limitations on the input, state and/or output variables are added as mathematical constraints in the formulation of the problem. The MPC methodology follows a receding horizon approach, i.e. only the first element of the sequence of control actions is actually implemented. In the next time instant, the state of the system is sampled again and the optimization problem is formulated and solved again, taking into account new available information. In standard MPC the performance criterion is the deviation of the future controlled process variables from a reference trajectory. In Fig. 2 the MPC control strategy is depicted.

3. Demand response strategies and controller synthesis

Our main concern in this work is to provide more flexibility to the consumers in order for them to participate more actively in the balancing effort. For this purpose we developed two DR techniques which give the consumers the option to move or shift energy loads in time. These options can be used either alone or in combination with using storing energy devices. However, it should be noted that energy storage is not always feasible due to cost and/or space limitations. Additionally, storage of energy implies energy losses and maintenance cost. Using shiftable loads, consumers actually postpone an energy demand and consume it at a later time by avoiding extra storage costs. In order to formulate the MPC problem at each discrete time instant k we need to take a decision, we are introducing the following notation:
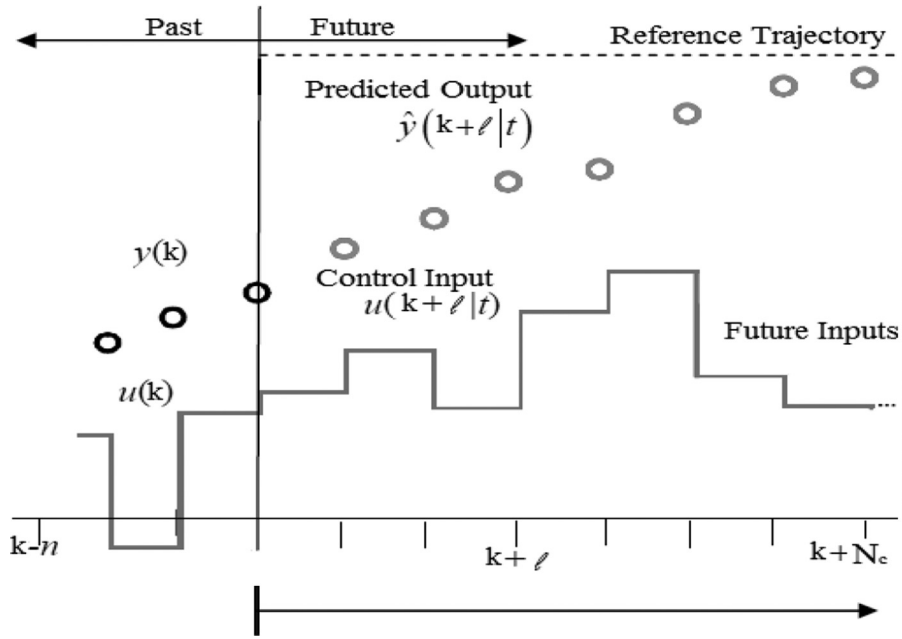
Fig. 2. The MPC control strategy.

3.1. Uncontrollable consumption

$$\bar{P}_i(k) = m_i \left\{ \overbrace{\begin{bmatrix} \bar{p}_{i,1}(k|k) & \cdots & \bar{p}_{i,1}(k+N_c|k) \\ \vdots & \ddots & \vdots \\ \bar{p}_{i,m_i}(k|k) & \cdots & \bar{p}_{i,m_i}(k+N_c|k) \end{bmatrix}}^{N_c+1} = \overbrace{\begin{bmatrix} \bar{p}_i(k|k) & \cdots & \bar{p}_i(k+N_c|k) \end{bmatrix}}^{N_c+1}, \ i=1,\dots,n_B \tag{10}$$

The matrix $\bar{P}_i(k)$ contains the uncontrollable consumptions for each consumer under BPP i for the current and the next N_c time periods which are assumed to be fully and precisely known. We use the notation $\bar{p}_{i,c}(k+l|k)$, $c=1,\dots,m_i$, $l=0,\dots,N_c$ to represent the uncontrollable consumption of consumer c under BPP i during period l after current time instant k. $\bar{p}_i(k+l|k)$ collects in a column vector uncontrollable consumptions of all consumers under BPP i during period l after current time instant k.

3.2. Controllable consumption

$$\dot{P}_i(k) = m_i \left\{ \overbrace{\begin{bmatrix} \dot{p}_{i,1}(k|k) & \cdots & \dot{p}_{i,1}(k+N_c|k) \\ \vdots & \ddots & \vdots \\ \dot{p}_{i,m_i}(k|k) & \cdots & \dot{p}_{i,m_i}(k+N_c|k) \end{bmatrix}}^{N_c+1} = \begin{bmatrix} \dot{p}_i(k|k) & \cdots & \dot{p}_i(k+N_c|k) \end{bmatrix}, \ i=1,\dots,n_B \tag{11}$$
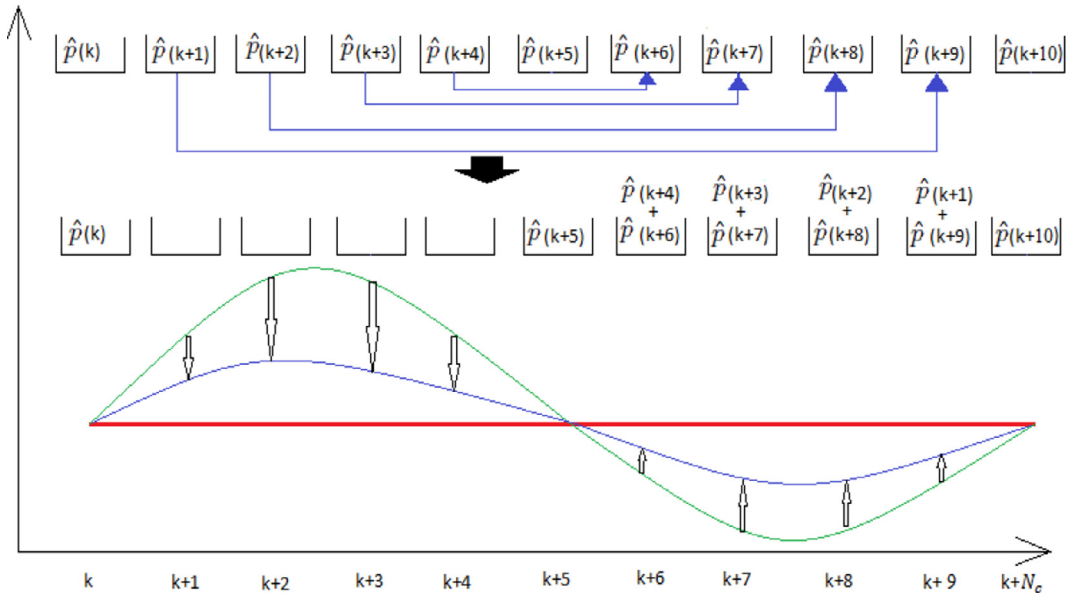
Using analogous notation to the uncontrollable consumption, the matrix $\dot{p}_i(k)$ contains the controllable consumptions, which are unknown continuous variables restricted by Eqs. (2)–(4), i.e.:

$$e_i(k+l|k) = D_i e_i(k+l-1|k) + \dot{p}_i(k+l|k), \ l=1,\dots,N_c \ i=1,\dots,n_B \tag{12}$$

$$0 \le e_i(k+l|k) \le e_i^{max}, \ l=1,\dots,N_c \ i=1,\dots,n_B \tag{13}$$

$$p_i^{min} \le \dot{p}_i(k+l|k) \le p_i^{max}, \ l=1,\dots,N_c \ i=1,\dots,n_B \tag{14}$$

$e_i(k|k)$ is the current vector for stored energy quantities under BRP i which is known.

Fig. 3. Schematic representation of Demand response 1. Red line depicts the desired value of the consumption q_{spot}, blue line is the original consumption and green line is the consumption after DR- 1. (For interpretation of the references to colour in this figure legend, the reader is referred to the web version of this article.)

3.3. Hourly shiftable consumption - Demand response 1 (DR1)

In this strategy we assume that consumers have the ability to shift in time a certain amount of their hourly energy needs. In addition, we assume that this load shifting is limited by the control horizon of the MPC controller and can happen only forward in time. The following matrices are formed for each BRP i at time instant k:

$$\hat{P}_i(k) = m_i \left\{ \begin{bmatrix} \hat{p}_{i,1}(k|k) & \dots & \hat{p}_{i,1}(k+N_c|k) & \times & B_{i,1} \\ & & & & \vdots \\ \hat{p}_{i,m_i}(k|k) & \dots & \hat{p}_{i,m_i}(k+N_c|k) & \times & B_{i,m_i} \end{bmatrix} = \begin{bmatrix} \hat{p}_i(k|k) & \dots & \hat{p}_i(k+N_c|k) \end{bmatrix}, \; i = 1, \dots, n_B \quad (15)$$

For every consumer under BRP-i, a square binary upper triangular matrix $B_{i,c} \in \mathbb{R}^{N_c+1 \times N_c+1}$, $c = 1, \dots, m_i$ is introduced. Therefore all elements of the main diagonal together with the elements above are binary decision variables, while all the elements below the main diagonal are forced to zero. We further restrict the values of matrices $B_{i,j}$ by the following inequality, which requires only one element of each row to take the value of 1, while all other elements are 0:

$$\sum_{j=0}^{N_c} B_{i,c}(l, j) = 1 \, , \qquad l = 0, \dots, N_c, \qquad c = 1, \dots, m_i \tag{16}$$

For row l, the column j for which $B_{i,c}(l, j)$ is equal to 1, actually means that the shiftable load of consumer c originally planned for period l will be shifted to period j within the control horizon N_c. Obviously if l coincides with j, no load shift will occur. The fact that all binary matrices are upper diagonal actually means shiftable loads are not allowed to be shifted backwards in time.

In Fig. 3 we can see a schematic representation of the proposed DR1 technique. The vertical axis represents the energy consumption, while the horizontal one represents time instants. The red line refers to q_{spot}, the green line to the actual consumption and the blue one to the consumption after the implementation of DR1.

3.4. Shiftable consumption following a pattern - Demand response 2 (DR2)

This methodology concerns energy consumptions which maintain a specific pattern in time. A typical example is the washing machine [23], which follows a specific energy consumption pattern that can be shifted in time, but cannot be interrupted. In order to capture this kind of energy demands, we made use of logical expressions. More details on how hybrid optimization problems are designed, formulated and solved can be found in [28, 29] and [30]. To start with, we assume that consumer c under BRP i has a consumption which maintains a specific pattern and can be shifted in time. This pattern is denoted as $\breve{p}_{i,c} = [\breve{p}_{i,c}(1), \; \breve{p}_{i,c}(2), \; \dots, \; \breve{p}_{i,c}(T_{d,c})]$ where $T_{d,c}$ is the duration in time periods of this consumption.

Let $\delta_{i,c,\,1} = [\delta_{i,c,\,1}(0),\ \delta_{i,c,\,1}(1),\ \ldots,\ \delta_{i,c,\,1}(N_c)]$ be a vector of binary variable indicating the starting period of the pattern for consumer c. Obviously, only one element of this vector must be equal to 1, while all other entries should be zero. It must be guaranteed that once the pattern begins, it must be consumed within the given time horizon N_c. These limitations are enforced by the following equations:

$$\delta_{i,c,1}(l) = 0, \quad l = N_c - T_{d,c} + 2, \ldots, N_c, \quad i = 1, \ldots, n_B, \quad c = 1, \ldots, m_i \tag{17}$$

$$\sum_{l=0}^{N_c} \delta_{i,c,1}(l) = 1, \ i = 1, \ldots, n_B, \ c = 1, \ldots, m_i \tag{18}$$

Now we introduce an additional set of $T_d - 1$ binary vectors $\delta_{i,c,\,j} = [\delta_{i,c,\,j}(0),\ \delta_{i,c,\,j}(1),\ \ldots,\ \delta_{i,c,\,j}(N_c)], j = 2, \ldots, T_{d,c}$ each one indicating the period in the time horizon where the j'th component of the pattern will be scheduled. Each one of these vectors contains only one element equal to 1 and is produced by shifting the values of the previous vector by one position to the right, while the first element becomes zero:

$$\left[\delta_{i,c,j}(0), \delta_{i,c,j}(1),\ \delta_{i,c,j}(2), \ldots,\ \delta_{i,c,j}(N_c)\right] = \left[0,\ \delta_{i,c,j-1}(0), \delta_{i,c,j-1}(1) \ldots,\ \delta_{i,c,j-1}(N_c - 1)\right], \ j = 2, \ldots, T_{d,c} \tag{19}$$

The following matrices are then formed for each BRP i at time instant k containing the prediction for the flexible consumption under DR2 strategy:

$$\breve{P}_i(k) = m_i \left\{ \overbrace{\begin{bmatrix} \sum_{j=1}^{T_{d,1}} (\delta_{i,1,j}\breve{p}_{i,1}(j)) \\ \vdots \\ \sum_{j=1}^{T_{d,m_i}} \left(\delta_{i,m_i,j}\breve{p}_{i,m_i}(j)\right) \end{bmatrix}}^{N_c+1} = \begin{bmatrix} \breve{p}_i(k|k) & \ldots & \breve{p}_i(k+N_c|k) \end{bmatrix}, \ i = 1, \ldots, n_B \tag{20}$$

By adding the aforementioned matrices, a new matrix is formulated containing the predictions of the total energy consumption during the prediction horizon for all consumers under BRP i:

$$P_i(k) = \begin{bmatrix} p_i(k|k) & \ldots & p_i(k+N_c|k) \end{bmatrix} = \tilde{P}_i(k) + \bar{P}_i(k) + \hat{P}_i(k) + \breve{P}_i(k), \ i = 1, \ldots, n_B \tag{21}$$

3.5. Controller synthesis

Based on the above notation the following centralized MPC (CMPC) optimization problem is formulated at each time instant k

3.5.1. Centralized MPC (CMPC)
1. Observe current state $e(k)$ and solve the optimization problem:

$$
\begin{aligned}
&minimize \ \sum_{l=0}^{N_c} \Phi(k+l|k) \\
&s.t.\ \text{Eqs.}(12),\ (13),\ (14),\ (16),\ (17),\ (18),\ (20) \\
&\text{And additionally :} \\
&t_i(k+l|k) = R_i p_i(k+l|k) \qquad l = 1, \ldots, N_c \quad i = 1, \ldots, n_B \\
&f(k+l|k) = \sum_{i=1}^{n_B} t_i(k+l|k) \qquad l = 1, \ldots, N_c \\
&f(k+l|k) \le f^{max} \qquad\qquad l = 1, \ldots, N_c
\end{aligned}
\tag{22}
$$

where:

$$\Phi(k+l|k) = \sum_{i=1}^{n_B} h_i\left(q_{bal,i}(k+l|k)\right) = \sum_{i=1}^{n_B} \left\| \mathbf{1}^T p_i(k+l|k) - q_{spot,i}(k+l) \right\|_2^2$$

where, $p_i(k+l|k)$ is given by Eq. (21). $\Phi(k+l|k)$ is used as an intermediate variable and represents the predicted sum of squared errors between the total consumptions of energy and the amounts of energy bought at the day-ahead-market over all BRPs at the lth time period in the control horizon. The decision variables involved in the CMPC optimization problem are the continuous variables $e_i(k+1: k+N_c)$ and $\tilde{p}_i(k : k+N_c)$ and the binary variables included in $\hat{P}_i(k),\ \breve{P}_i(k)$.

2. From the solution, apply the part referring to current time instant.
3. Increase k by one and repeat from step 1.

CMPC considers the coupled constraint $f(k+l|k) \leq f^{max}$ and solves the problem centrally. It assumes that BRPs share information such as current state of consumers and consumption prediction profiles, which is quite unrealistic. In this paper, we decouple the originally centralized problem using dual decomposition [31]. For this purpose we introduced the Lagrange multipliers $\lambda(k+l|k)$ (named shadow prices in [20]). The partial Lagrangian of the problem is:

$$L(\eta, \lambda) = \sum_{i=1}^{n_B} \sum_{l=0}^{N_c} h_i\big(q_{bal,i}(k+l|k)\big) + \sum_{l=0}^{N_c} \lambda^{\mathrm{T}}(k+l) * (f(k+l|k) - f^{max}) \tag{23}$$

where η is a vector containing all the decision variables of the problem formulated at time instant k. Now our problem is separable, so we can minimize over each BRP separately given the dual variable λ in order to find the dual function, $g(\lambda) = \sum_{l=1}^{n_B} g_i(\lambda)$, of our original (master) problem. To find $g_i(\lambda)$ we solve the following subproblem:

$$g_i(\lambda) = \min_{\eta_i} \sum_{l=0}^{N_c} h_i\big(q_{bal,i}(k+l|k)\big) + \lambda^{\mathrm{T}}(k+l) * t_i(k+l|k) \tag{24}$$

To ensure the convergence of the dual problem we made use of an iterating method, namely the subgradient method [32]. A subgradient of the negative dual function – g_i at λ is given by $\bar{t}_i(k+l)$, where $\bar{t}_i(k+l)$ is the solution of subproblem (24).

The summation of all the above $g_i(\lambda)$ of each BRP gives the total subgradient $g(\lambda)$ of Eq. (23). Then we solve the original problem (22) separately for each BRP by substituting the originally coupled constraint $f(k+l|k) \leq f^{max}$ by $t_i(k+l|k) \leq \bar{t}_i(k+l|k)$. This Distributed MPC (DMPC) approach is described next:

3.5.2. Distributed MPC (DMPC)
1. DSO initializes the shadow prices ($\lambda(k)=0$ or $\lambda(k)=\lambda(k-1)$).
2. Repeat
   a) DSO gives each BRP the shadow prices
   b) Each BRP $i=1, \ldots, n_B$ solves the problem:

$$minimize \quad \sum_{l=0}^{N_c} \big(h_i\big(q_{bal,i}(k+l|k)\big) + \lambda^{\mathrm{T}}(k+l) * t_i(k+l|k)\big)$$
$$s.t. \quad \text{Eqs.} (12), (13), (14), (16), (17), (18), (20) \text{ applied only for BRP } i \tag{25}$$
$$\text{Additionally :}$$
$$t_i(k+l|k) = R_i p_i(k+l|k) \ l = 1, \ldots, N_c$$

   c) Each BRP reports partial flows $\bar{t}_i(k+l|k)$ to the DSO. DSO checks for capacity violations $s(k+l|k) = \sum_{i=1}^{n_B} t_i(k+l|k) - f^{max}$.
3. DSO updates shadow prices using projected subgradient method $\lambda(k+l|k) = \max(0, \ \lambda(k+l|k) + a * s(k+l|k))$.
4. Until $\max(s(k+l|k)) \leq \varepsilon$ or maximum number of iterations reached.
5. Maximum partial flows $t_i^{max}(k+l|k)$ are communicated to the BRPs:

$$t_i^{max}(k+l|k) = A_{i,l} * \bar{t}_i(k+l|k) \tag{26}$$

   where, $A_{i,l} \in R^{n_L \times n_L}$ is a diagonal matrix and its jth element is $f_j^{max} / (\sum_{i=1}^{n_B} \bar{t}_i(k+l|k))_j$. This assures feasibility using backtracking.
6. Each BRP solves problem (25) adding the constraint $t_i(k+l|k) \leq t_i^{max}(k+l|k)$.
7. From the solution, apply the part referring to current time instant.
8. Increase k by one and repeat from step 1.

4. Simulation results

In this section we apply the control schemes described in Section 3 to the IEEE ELVTF, the topology of which is shown in Fig. 4. The low voltage test feeder is a radial distribution feeder with a base frequency of 50 Hz. The feeder is connected to the medium voltage (MV) system through a transformer at substation. In [26] the detailed description of the feeder can be found, as well as all the necessary data for simulation purposes.

The grid consists of two BRPs (BRP1 and BRP2), and fifty five consumers. BRP1 is responsible for all the consumers enclosed by the black polyline, whereas consumers enclosed by the red one are in the responsibility of BRP2. As it can be seen in Fig. 4, consumers C8 (under BRP1) and C12 (under BRP2) share the same distribution line. As a result, congestion of that line might occur due to conflicting interests between the two BRPs. Since consumption data are provided in one-minute time resolution, we summed up all consumptions during one hour for every consumer and hourly energy consumption data were derived for the proposed control strategy which uses a time period of one hour.
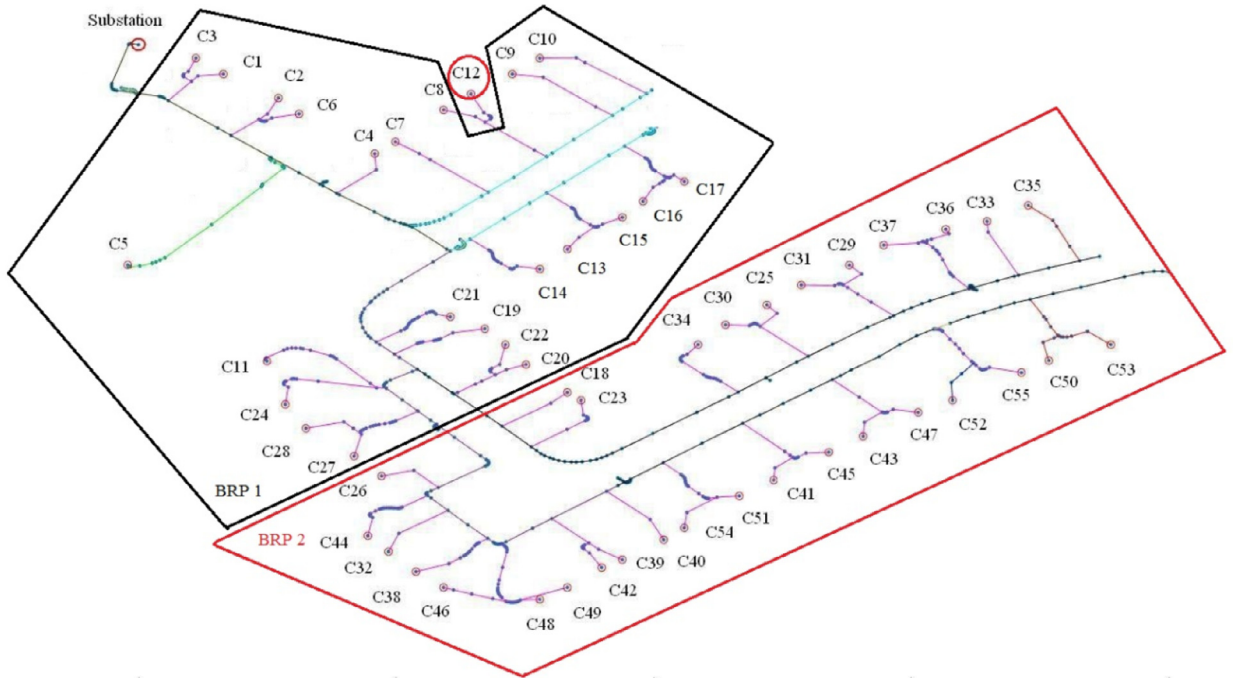
Fig. 4. The IEEE LVTF topology. It consists of two BRPs and 55 consumers. (For interpretation of the references to colour in this figure, the reader is referred to the web version of this article.)

The following assumptions have been made:

- Consumers C1, C2, C5, C8, C13, C17, C20 and C21 under BRP1 and consumers C12, C29, C30, C37, C39, C45, C47, C48, C50 C52 and C53 under BRP can store energy and move 10% of their total hourly energy needs at each time period to subsequent periods within the 24-h time framework.
- The energy storage capacities of flexible consumers is set at 100 kWh with the exception of consumers C8 and C12 for which a 200 kWh capacity is assumed.
- Drain loses for energy storage device are 0.8 and 0.99 for flexible BRP1 and BRP2 consumers respectively.
- Consumers C4, C10 and C24 under BRP1 have the option to move the following load patterns, all taking three consecutive hour periods to complete: $\breve{p}_{1,4} = [60\ \ 15\ \ 10]$, $\breve{p}_{1,10} = [40\ \ 20\ \ 80]$, $\breve{p}_{1,24} = [30\ \ 10\ \ 20]$.
- Similarly, consumers C33, C35 and C49 under BRP2 have the option to move the following load patterns over three consecutive hour periods: $\breve{p}_{2,33} = [30\ \ 80\ \ 100]$, $\breve{p}_{2,35} = [60\ \ 50\ \ 30]$, $\breve{p}_{2,49} = [70\ \ 10\ \ 30]$.
- The rest of the consumers under BRP1 and BRP2 are non-flexible consumers (they cannot store or move energy loads).
- Only the active power is considered for control purposes in the form of energy consumed by the consumers in the hour time scale.
- Distribution line power loses are neglected.
- Maximum energy flows f^{max} were set to the maximum amount of energy transferred through them plus a safety factor of 5%.

Figs. 5 and 6 show in an hourly basis, the energy purchased at the DAM by BRP1 and BRP2 (denoted by $q_{spot,1}$ and $q_{spot,2}$ respectively), as well as the predicted consumptions for the two BRPs for the next 24-h period.

The energy purchased by BPRs is based on predictions of energy prices in the DAM. Obviously, there are mismatches between the purchased energy patterns and the predicted hourly energy consumptions. BRPs are buying less energy during peak energy hours and more energy when the demand is low. This is because BRPs count on consumption flexibility and DR strategies to shift energy loads and produce an actual consumption profile which matches as much as possible the q_{spot} patterns.

Two different scenarios were examined, assuming that the energy consumptions over the next 24-h period are precisely known. In the first scenario, energy storage is the only demand response option. In the second scenario, all demand response strategies are allowed (energy storage, shifting energy demand of hourly duration, shifting movable energy patterns). The results are compared to the base case shown in Figs. 5 and 6 where no demand response actions are allowed.

In both scenarios, we applied CMPC and DMPC in order to compare the results between the two control schemes. The simulations were performed in the programming environment of MATLAB® using a prediction horizon Np = 10 and a control
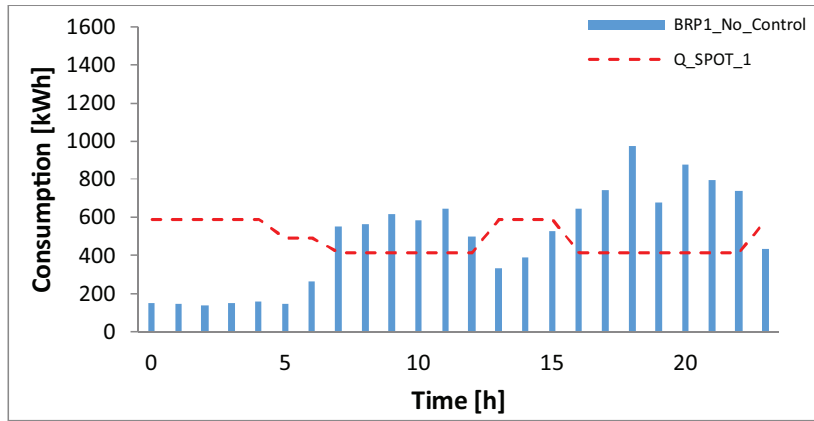
Fig. 5. Total consumption (blue solid line) and $q_{spot,1}$ (red dashed line) for BRP1. (For interpretation of the references to colour in this figure legend, the reader is referred to the web version of this article.)
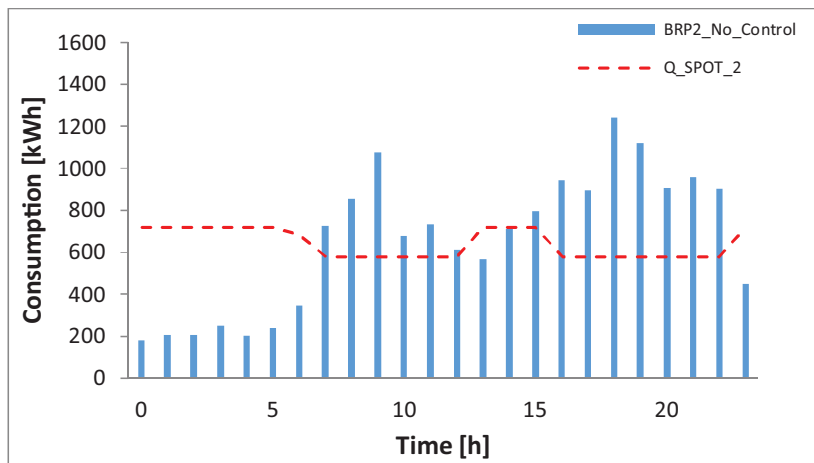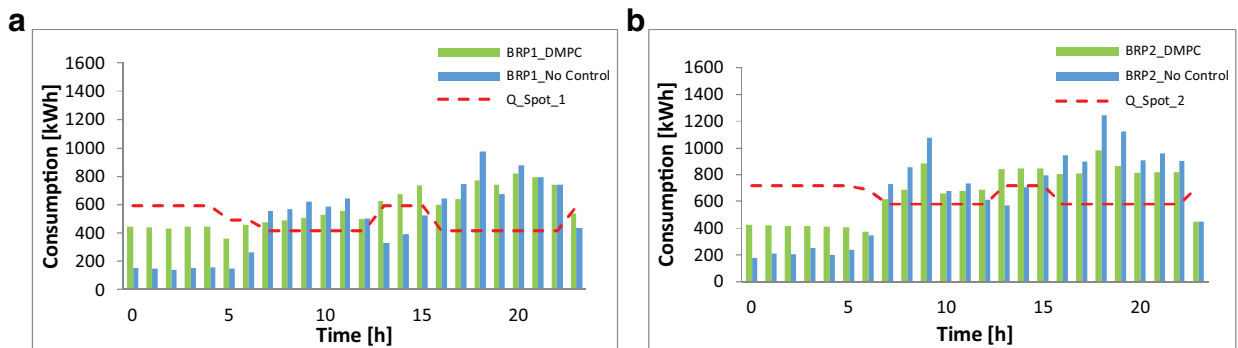

Fig. 6. Total consumption (blue solid line) and $q_{spot,2}$ (red dashed line) for BRP2. (For interpretation of the references to colour in this figure legend, the reader is referred to the web version of this article.)

Fig. 7. Total consumption distribution for scenario 1: BRP1 (a) and BRP2 (b). (For interpretation of the references to colour in this figure, the reader is referred to the web version of this article.)

horizon of the same length. The optimization problems were formulated using the YALMIP® ([33]) optimization toolbox and solved using MOSEK® 7.1 ([34]).

Figs. 7 and 8 present graphically the total energy consumptions for the two BRPs after the application of DMPC. CMCP produces almost identical results as it will be shown briefly later in the paper (Tables 2 and 4). The green bars represent the hourly energy consumptions after the application of DMPC, whereas blue bars correspond to the base case, which is shown again in the figures for comparison purposes. As shown in Fig. 9, in both scenarios, the storage devices are increasing
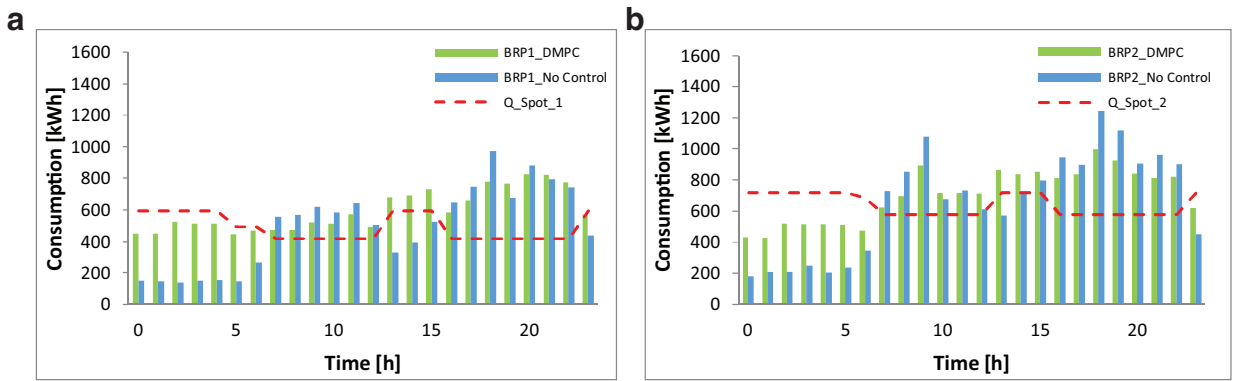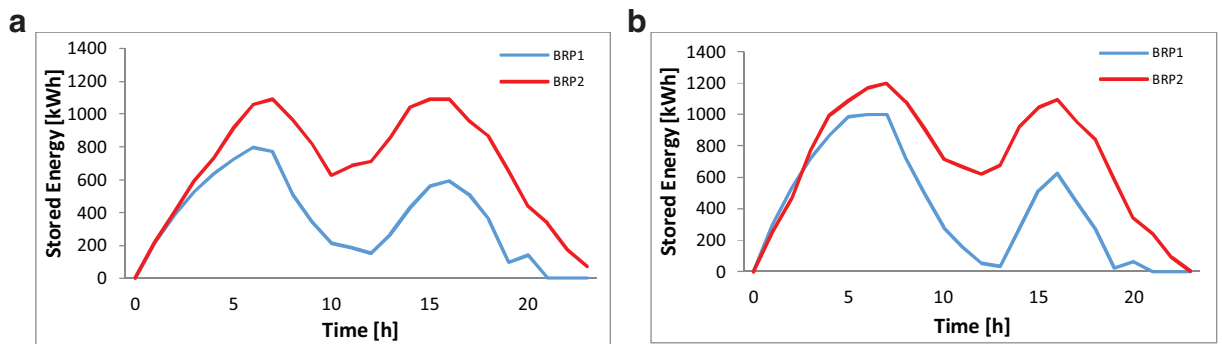
Fig. 8. Total consumption distribution for scenario 2: BRP1 (a) and BRP2 (b). (For interpretation of the references to colour in this figure, the reader is referred to the web version of this article.)

Fig. 9. Energy stored in storage devices of flexible consumers under BRP1 and BRP2 over the 24-h period. (For interpretation of the references to colour in this figure, the reader is referred to the web version of this article.)

Table 1
Consumption of energy patterns.

Consumer	Consumption of energy patterns	
	Time periods (Base case)	Time periods DMPC
C4	[18 19 20]	[2 3 4]
C10	[9 10 11]	[3 4 5]
C24	[17 18 19]	[2 3 4]
C33	[17 18 19]	[3 4 5]
C35	[8 9 10]	[4 5 6]
C49	[18 19 20]	[4 5 6]

Table 2
Balancing energy comparison between CMPC and DMPC for the two different scenarios for precisely known energy consumptions.

Scenario	Total balancing energy – base case (MWh)	Total balancing energy – CMPC (MWh)	Total balancing energy – DMPC (MWh)	Difference between CMPC and DMPC (%)	DMPC deviation from base case (%)
1	14.84	9.30	9.30	≈ 0	−59.57
2	14.84	8.72	8.74	0.23	−69.79

the stored energy levels in periods when energy prices in the DAM are low and release energy when prices are high and this reduces the discrepancy between planned and actual energy purchases. In the second scenario the balancing energy is reduced further, because controllers move energy loads from peak hours to hours of lower traffic of the grid. This is illustrated clearly in Table 1, which shows that all energy patterns are transferred to the beginning of the 24-h period, where energy demands are low.

The produced optimal values of the balancing energy objective function computed over the 24-h period are summarized in Table 2. They are compared with the base case, where neither energy storage nor shifting of consumption is possible. Reduction of balancing energy is almost 60% in the first scenario and is improved in the second scenario, where we provide
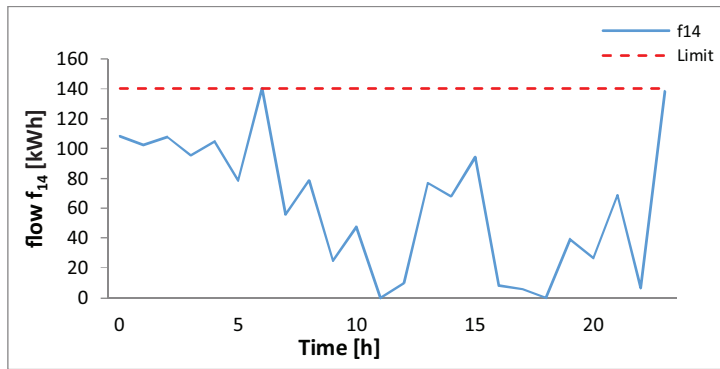
Fig. 10. Total energy flow through distribution line 14 for scenario 2 (blue solid line) and its upper limit value (red dashed line). (For interpretation of the references to colour in this figure legend, the reader is referred to the web version of this article.)

Table 3
Partial flow variations during the iterations of the subgradient method for distribution line 14 and $k = 7$ for scenario 2.

j	1	2	3	4	5	6	7	8	9	10
$\bar{t}_1$	129.33	129.33	129.39	127.58	126.96	126.85	126.83	126.83	126.83	126.83
$\bar{t}_2$	18.42	18.42	18.42	18.42	18.42	18.42	18.42	18.42	18.42	18.42
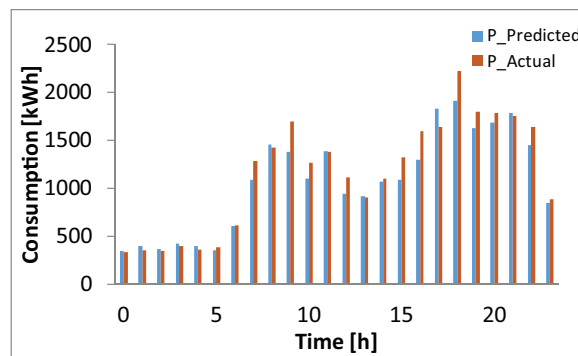
Fig. 11. Predicted and actual consumption profiles, when uncertainty is considered in energy predictions. (For interpretation of the references to colour in this figure, the reader is referred to the web version of this article.)

additional flexibility and demand response options. CMPC and DMPC produce identical results in the first scenario, whereas in the second scenario the difference is negligible.

The ability of the proposed control method to avoid congestion is illustrated in Fig. 10, which shows the total flow through the distribution line 14 using the DMPC approach in scenario 2. It is clear that the flow meets but does not exceeds its upper capacity at $k = 7$. Congestion did not occur, thanks to the introduction of the shadow prices. During the busy hours, DSO detects violation of this line due to conflicting interests among the BRPs and increases the energy prices (shadow prices) of this specific distribution line. Accordingly, BRPs respond to this price change by decreasing their demands transferred through this particular line. Table 3 presents the partial flows calculated iteratively by the subgradient method, while applying DMPC at time instant $k = 7$. It can be clearly seen that BRP2 is not reducing its demand in contrast to BRP1. This is due to better quality of storage facilities of BRP2. We can also observe that even after the eighth iteration of the subgradient method the summation of total partial flows for line 14 is above the upper limit, which is 140.25 kWh for this particular line. Backtracking, in step 5 of DMPC, is used to avoid infeasibility of the optimization problem.

Next, we executed all simulations again, by now considering uncertainties in the predicted consumptions. More specifically, we assumed that the actual consumptions are the ones shown in Figs. 5 and 6, but the predicted ones which are presented to the control schemes are different, as shown in Fig. 11. The differences have been produced by random number generations from a uniform distribution.

Table 4 summarizes the results when uncertainty in energy predictions is considered. We observe that the application of both CMPC and DMPC again reduces considerably the total balancing energy compared to the base case. Compared to Table 2, the results for scenario 1 are identical, while for scenario 2 they are slightly deteriorated. This happens because due to uncertain predictions, the patterns are now always placed in the optimal time slots.

Table 4
Balancing energy comparison between CMPC and DMPC for the two different scenarios when uncertainties are assumed in consumption predictions.

Scenario	Total balancing energy – base case (MWh)	Total balancing energy – CMPC (MWh)	Total balancing energy – DMPC (MWh)	Difference between CMPC and DMPC (%)	DMPC deviation from base case (%)
1	14.84	9.3	9.3	≈ 0	−59.57
2	14.84	8.85	9.01	1.75	−64.71

Table 5
Computational Times for executing the 24-h simulation.

	Scenario 1				Scenario 2			
	DMPC		CMPC		DMPC		CMPC	
	Unc.*	Perf.**	Unc.*	Perf.**	Unc*	Prec**	Unc*	Prec**
Time (s)	80.7	287.8	16.8	15.6	816.9	571.9	65.5	66.3

* Uncertain consumption prediction.
** Perfect consumption prediction.
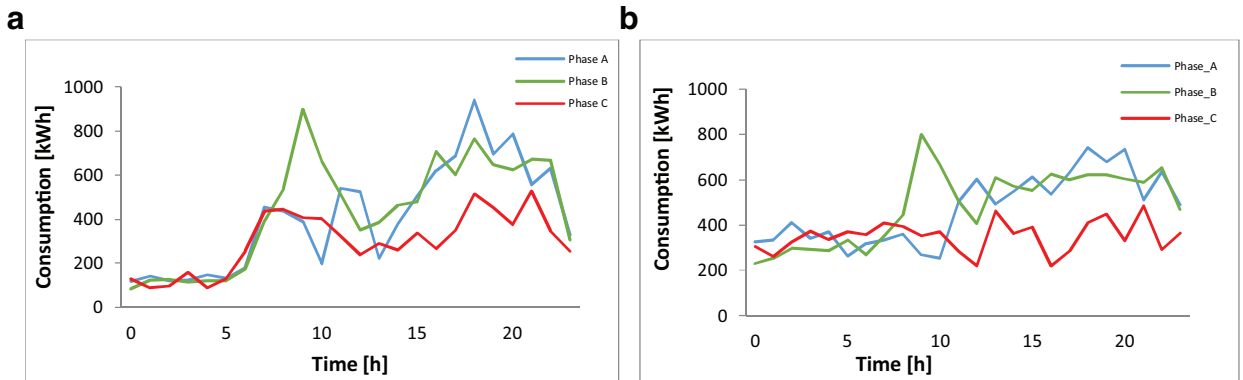
Fig. 12. Three phases energy consumption profiles in the base case (a) and in scenario 2 (b) for precisely known energy consumptions. (For interpretation of the references to colour in this figure, the reader is referred to the web version of this article.)

Table 5 presents the computational time needed to produce the full 24-h simulation in a Laptop with Intel Core i7-5500 U at 2.40 GHz and 8 GB RAM. As it was expected, the required computational time is increased with the complexity of demand response strategies. DMPC clearly need more computational time compared to CMPC, obviously because of its iterative strategy. However, even in the worst case (DMPC in scenario 2 with uncertainties) the solution time is less than 14 min, which means that only a few seconds are required to calculate the optimal control input at each period. Taking into account that decisions are made every hour, even this worst case solution time is acceptable in a realistic problem as the one used in the paper.

Although consumers are regarded as single-phase in the formulation of the MPC schemes, the IEEE LVTF is a three-phase system and it gives all the necessary information to evaluate the impact of the proposed control schemes from the three-phase point of view. According to [26] consumers C_1, C_3, C_4, C_5, C_9, C_{14}, C_{20}, C_{21}, C_{22}, C_{25}, C_{29}, C_{30}, C_{31}, C_{34}, C_{46}, C_{48}, C_{49}, C_{51}, C_{52}, C_{54} and C_{55} are connected to phase A, consumers C_2, C_6, C_7, C_{10}, C_{11}, C_{13}, C_{15}, C_{23}, C_{26}, C_{35}, C_{36}, C_{37}, C_{38}, C_{40}, C_{41}, C_{44}, C_{45}, C_{50}, and C_{53} are connected to phase B, while consumers C_8, C_{12}, C_{16}, C_{17}, C_{18}, C_{19}, C_{24}, C_{27}, C_{28}, C_{32}, C_{33}, C_{39}, C_{42}, C_{43} and C_{47} are connected to phase C. In Fig. 12(a), the total consumption for the three phases of the system is depicted for the base case, where no demand response is possible. The unbalance in the three phases is obvious, especially in time interval 9. More specific, the sudden pick of phase B during that time interval may lead to voltage issues of the system. Fig. 12(b) depicts the same type of graph when DMPC is used in scenario 2. The energy consumption lines corresponding to the three phases are now smoother, although this objective has not been taken into consideration during the formulation of the optimization procedure. Especially for phase B in the time interval 7–10, the pick energy consumption has been reduced by 12.35% in the case of perfectly known consumption profiles and by 12.76% in the presence of uncertainty.

As a next step, we examined the option of extending the formulation of the CMPC and DMPC problems, so that energy differences among the three phases are bounded using hard constraints. In this case, the following constraints are incorporated into the optimization algorithms, in both the CMPC and the DMPC formulations:

$$\left(\sum_A p_i(k+l|k) - \sum_B p_i(k+l|k) \right) \le p_{i,|A-B|}^{max} \ l = 1..N_c \ i = 1..n_B \tag{27}$$

Table 6
Maximum allowable differences between the three phases for both the BRPs and the scenarios.

Parameter		Value (kWh)	
		BRP1	BRP2
Scenario 1	$p_{i,|A-B|}^{max}$	200	260
	$p_{i,|A-C|}^{max}$	150	200
	$p_{i,|B-C|}^{max}$	180	280
Scenario 2	$p_{i,|A-B|}^{max}$	180	160
	$p_{i,|A-C|}^{max}$	150	180
	$p_{i,|B-C|}^{max}$	180	250
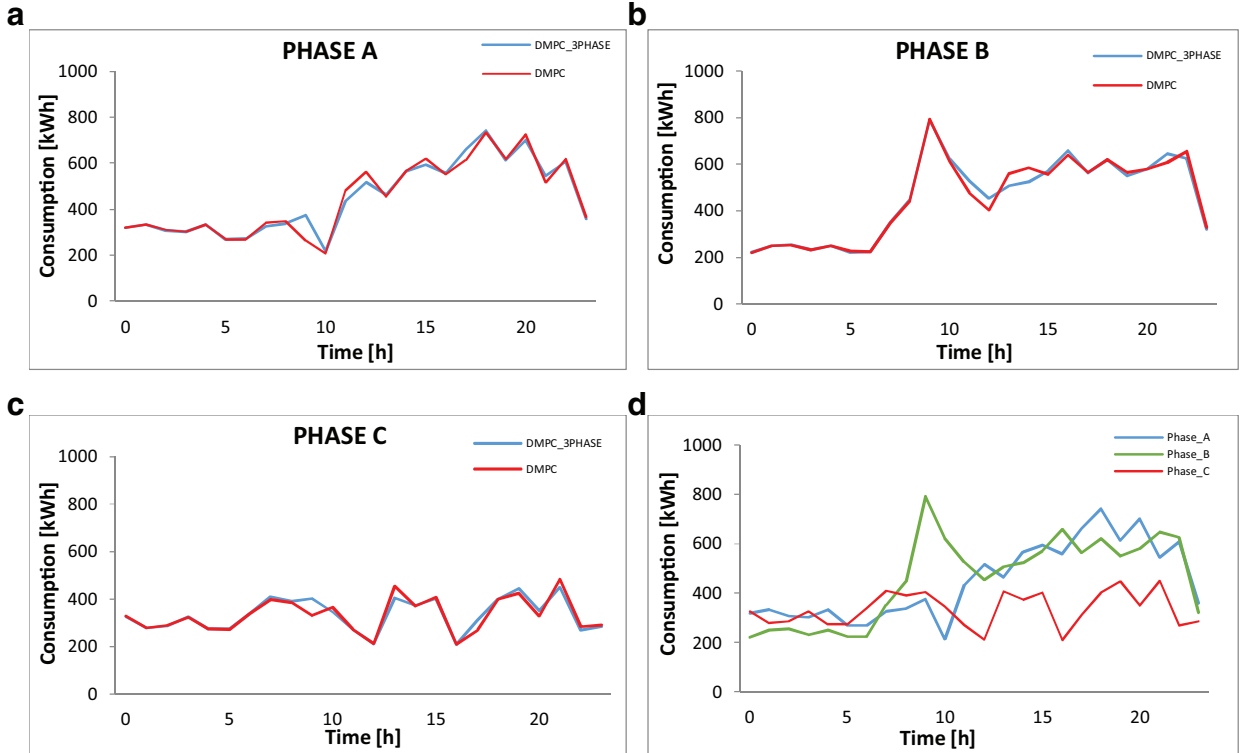
Fig. 13. Three phase consumption patterns between DMPC (red line) and DMPC_3PHASE (blue line) (a–c) in scenario 1. Total consumption profile for DMPC in scenario 1 (d). (For interpretation of the references to colour in this figure legend, the reader is referred to the web version of this article.)

$$\left(\sum_A p_i(k+l|k) - \sum_C p_i(k+l|k) \right) \le p_{i,|A-C|}^{max} \ l = 1..N_c \ i = 1..n_B \tag{28}$$

$$\left(\sum_B p_i(k+l|k) - \sum_C p_i(k+l|k) \right) \le p_{i,|B-C|}^{max} \ l = 1..N_c \ i = 1..n_B \tag{29}$$

where $\sum_A p_i(k+l|k)$, $\sum_B p_i(k+l|k)$, $\sum_C p_i(k+l|k)$ are the summations of all consumers of BRP i at time instance $k+l$ connected to phases A,B,C respectively and $p_{i,|A-B|}^{max}$, $p_{i,|A-C|}^{max}$, $p_{i,|B-C|}^{max}$ are the bounds on energy differences.

We performed all the simulations again for both scenarios and for both CMPC and DMPC when no uncertainties are considered and by additionally taking into account Eqs. (27)–(29) with the bounds shown in Table 6. Notice that by further decreasing the bounds on energy differences among the three phases, the optimization problems are infeasible. For easy comparison with the previous results, these simulations are named CMPC_3PHASE and DMPC_3PHASE.

In Fig. 13 (a)–(c) the comparison between the DMPC and DMPC_3PHASE for scenario 1 is shown. No major differences are observed, but it is clear that during the 9th interval there is an effort to increase consumption in phases A and C and reduce the difference from consumption in phase B.

The balancing energy results for CMPC_3PHASE and DMPC_3PHASE are presented in Table 7. We observe that the incorporation of the additional constraints on energy differences among the three phases resulted in slightly worse results (smaller deviations from base case) compared to the results shown in Table 2.

Table 7
Balancing energy comparison between CMPC_3PHASE and DMPC_3PHASE for the two different scenarios for precisely known energy consumptions.

Scenario	Total balancing energy – base case (MWh)	Total balancing energy – CMPC_3PHASE (MWh)	Total balancing energy – DMPC_3PHASE (MWh)	Difference between CMPC_3PHASE and DMPC_3PHASE (%)	DMPC_3PHASE deviation from base case (%)
1	14.84	9.43	9.43	≈ 0	−57.40
2	14.84	9.05	8.80	2.89	−68.62

5. Conclusion and future work

In this paper, centralized and distributed MPC methodologies were developed in order to address major issues arising in the daily operation of the distribution grid, namely congestion of distribution lines and the balancing energy. The proposed control scheme should be considered as an intermediate control layer in a hierarchical control configuration, which computes the optimal steady state of the system under consideration or sends optimal set points to the subsequent control layers.

Demand respond strategies were incorporated into the MPC formulation, by giving the options of shifting parts of the hourly energy loads or full energy patterns. The proposed control schemes were tested on the IEEE European Low Voltage Test Feeder, consisting of 73 distribution lines and 55 consumers. Only the active power was considered as a control parameter in the form of energy consumed (kWh) in the time scale of one hour. In addition, the inherent uncertainty of future energy prediction profiles was also taken into consideration in the form of disturbances to the actual consumption data which are provided by the LVTF.

The obtained results after the implementation of the proposed control algorithms, illustrated that flexible consumers can significantly contribute to the balancing efforts and energy consumption profiles are produced which are similar to those bought by BRPs in the DAM. As a result, the total energy consumption of the system maintains a "flatter" shape improving this way considerably the performance of the overall system in terms of energy cost and congestion management. Results for the three-phase system were also produced indicating that demand response strategies in coordination with the use of storage devices can reduce the large variations of a single phase, and at the same time "brings" closer the consumption profiles of the three phases of the system.

The time requirements of the proposed control methods are well within the acceptable ranges. In both scenarios, two different controllers were developed. On the one hand, the optimization problem was formed and solved centrally, assuming that a centrally located entity has complete knowledge of the entire system. In this case, the computational time spent by the controller on the optimization procedure was significantly lower, 16.8 s in scenario 1 and 66.3 s in scenario 2 were the worst performance for CMPC, compared to those of DMPC. But this centralized control approach has the huge disadvantage that every BRP should provide all the necessary information concerning its consumers, such as cost functions, states of flexible consumers, consumption predictions etc. In practice, this is very unlikely to happen due to the competitive nature of energy market. On the other hand, in a distributed control approach different BRPs do not have to share each other all the data as far as their consumers is concerned. The only information they have to communicate is their demands on the distribution lines in order for the DSO to compute the energy prices (shadow prices) in case of congestion due to conflicting interest among different BRPs sharing the same distribution line. In this case the control algorithm was slower compared to the centralized one in both the scenarios, but still acceptable. This happens because of the iteration procedure which has to be followed in order for the consumers to reach a consensus. Finally, we concluded that DMPC produces almost identical results compared to CMPC as the maximum deviation between the two was 2.89% in the worst case. Therefore, DMPC is the most suitable approach in the realistic situation, where BRPs do not share information with each other, which is the case in the energy market.

A full hierarchical control methodology is planned to be developed next, which will include voltage control and control of the reactive power of the system, in the time scale of 1 min, including the implementation of the method to the IEEE ELVTF system. Finally, a techno-economic assessment would be very useful in terms of economic viability of the proposed control strategy.

References

[1] D.Q. Mayne, J.B. Rawlings, C.V Rao, P.O.M Scokaert, Constrained model predictive control: stability and optimality, Automatica 36 (2000) 789–814, doi:10.1016/S0005-1098(99)00214-9.
[2] J.M. Maciejovski, Predictive Control with Constraints, Pearson Education Limited, Prentice Hall, London, 2002.
[3] A.N. Venkat, I.A. Hiskens, J.B. Rawlings, S.J. Wright, Distributed MPC strategies with application to power system automatic generation control, IEEE Trans. Control Syst. Technol. 16 (2008) 1192–1206, doi:10.1109/TCST.2008.919414.
[4] P.D. Christofides, R. Scattolini, D. Muñoz de la Peña, J. Liu, Distributed model predictive control: a tutorial review and future research directions, Comput. Chem. Eng. 51 (2013) 21–41, doi:10.1016/j.compchemeng.2012.05.011.
[5] A.N. Venkat, I.A. Hiskens, J.B. Rawlings, S.J. Wright, Distributed output feedback MPC for power system control, in: Proceedings of the 45th IEEE Conference on Decision & Control, San Diego, USA, 2006, pp. 4038–4045, doi:10.1109/cdc.2006.377176.
[6] J. Bendtsen, K. Trangbaek, J. Stoustrup, Hierarchical model predictive control for plug-and-play resource distribution, Lect. Notes Control Inf. Sci. 417 (2012) 339–358, doi:10.1007/978-1-4471-2265-4_15.
[7] P. Siano, Demand response and smart grids - a survey, Renew. Sustain. Energy Rev. 30 (2014) 461–478, doi:10.1016/j.rser.2013.10.022.

[8] E.M.G. Rodrigues, R. Godina, E. Pouresmaeil, J.R. Ferreira, J.P.S. Catalão, Domestic appliances energy optimization with model predictive control, Energy Convers. Manag. 142 (2017) 402–413, doi:10.1016/j.enconman.2017.03.061.

[9] M. Majidi, S. Nojavan, K. Zare, Optimal stochastic short-term thermal and electrical operation of fuel cell/photovoltaic/battery/grid hybrid energy system in the presence of demand response program, Energy Convers. Manag. 144 (2017) 132–142, doi:10.1016/j.enconman.2017.04.051.

[10] G. Gutiérrez-Alcaraz, J.H. Tovar-Hernández, C.N. Lu, Effects of demand response programs on distribution system operation, Int. J. Electr. Power Energy Syst. 74 (2016) 230–237, doi:10.1016/j.ijepes.2015.07.018.

[11] H.T. Haider, O.H. See, W. Elmenreich, Residential demand response scheme based on adaptive consumption level pricing, Energy 113 (2016) 301–308, doi:10.1016/j.energy.2016.07.052.

[12] X. Wu, X. Hu, X. Yin, C. Zhang, S. Qian, Optimal battery sizing of smart home via convex programming, Energy 140 (2017) 444–453, doi:10.1016/j.energy.2017.08.097.

[13] G.R. Aghajani, H.A. Shayanfar, H. Shayeghi, Demand side management in a smart micro-grid in the presence of renewable generation and demand response, Energy 126 (2017) 622–637, doi:10.1016/j.energy.2017.03.051.

[14] X. Wu, X. Hu, Y. Teng, S. Qian, R. Cheng, Optimal integration of a hybrid solar-battery power source into smart home nanogrid with plug-in electric vehicle, J. Power Sources 363 (2017) 277–283, doi:10.1016/j.jpowsour.2017.07.086.

[15] H. Verdejo, W. Escudero, W. Kliemann, A. Awerkin, C. Becker, L. Vargas, Impact of wind power generation on a large scale power system using stochastic linear stability, Appl. Math. Model. 40 (2016) 7977–7987, doi:10.1016/j.apm.2016.04.020.

[16] H.W. Lu, M.F. Cao, J. Li, G.H. Huang, L. He, An inexact programming approach for urban electric power systems management under random-interval-parameter uncertainty, Appl. Math. Model. 39 (2015) 1757–1768, doi:10.1016/j.apm.2014.09.018.

[17] A. Yousefi, T.T. Nguyen, H. Zareipour, O.P. Malik, Congestion management using demand response and FACTS devices, Int. J. Electr. Power Energy Syst. 37 (2012) 78–85, doi:10.1016/j.ijepes.2011.12.008.

[18] European Commission, Official journal of the European union l 335/1, Off. J. Eur. Union. 2009 (2002) L335/1-129, doi:10.3000/17252555.L_2009.335.eng.

[19] B. Biegel, J. Stoustrup, J. Bendtsen, P. Andersen, Model predictive control for power flows in networks with limited capacity, in: 2012 American Control Conference, Montreal, QC, Canada, 2012, pp. 2959–2964, doi:10.1109/acc.2012.6314854.

[20] B. Biegel, P. Andersen, J. Stoustrup, J. Bendtsen, Congestion management in a smart grid via shadow prices, IFAC Proc 45 (2012) 518–523, doi:10.3182/20120902-4-FR-2032.00091.

[21] B. Biegel, L.H. Hansen, J. Stoustrup, P. Andersen, S. Harbo, Value of flexible consumption in the electricity markets, Energy 66 (2014) 354–362, doi:10.1016/j.energy.2013.12.041.

[22] S. Huang, Q. Wu, H. Zhao, C. Li, Distributed optimization-based dynamic tariff for congestion management in distribution networks, IEEE Trans. Smart Grid. 10 (2019) 184–192, doi:10.1109/TSG.2017.2735998.

[23] G.K.H. Larsen, J. Pons, S. Achterop, J.M.A. Scherpen, Distributed MPC applied to power demand side control, in: 2013 European Control Conference (ECC), Zurich, Switzerland, 2013, pp. 3295–3300, doi:10.23919/ecc.2013.6669616.

[24] B.M. Houwing, R.R. Negenborn, B. De Schutter, Demand response with Micro-CHP systems, Proceedings of the IEEE 99 (1) (2011) 200–213. https://doi.org/10.1109/jproc.2010.2053831.

[25] J.M.A. Scherpen, Distributed supply-demand balancing and the physics of smart energy systems, Eur. J. Control. 24 (2015) 63–71, doi:10.1016/j.ejcon.2015.04.005.

[26] IEEE PES, IEEE European LV Test Feeder, (2016). http://sites.ieee.org/pes-testfeeders.

[27] J.B. Rawlings, D.Q. Mayne, Postface to "model predictive control: theory and design", Nob Hill Publishing, LLC, 2009.

[28] A. Bemporad, M. Morari, Control of systems integrating logic, dynamics, and constraints, Automatica 35 (1999) 407–427, doi:10.1016/S0005-1098(98)00178-2.

[29] T.M. Cavalier, P.M. Pardalos, A.L. Soyster, Modeling and integer programming techniques applied to propositional calculus, Comput. Oper. Res. 17 (1990) 561–570, doi:10.1016/0305-0548(90)90062-C.

[30] H.P. Williams, Model Building in Mathematical Programming, John Wiley & Sons, 2013.

[31] S. Boyd, L. Xiao, A. Mutapcic, J. Mattingley, Notes on decomposition methods, Stanford University D (2007) 1–36. http://www.core.org.cn/mirrors/Stanford/stanford/see.stanford.edu/materials/lsocoee364b/08-decomposition_notes.pdf.

[32] S. Boyd, L. Xiao, A. Mutapcic, Subgradient methods, Stanford University, 2003 Notes for EE392o. http://www.stanford.edu/class/ee392o/subgrad_method.pdf

[33] J. Lofberg, YALMIP: a toolbox for modeling and optimization in MATLAB, in: 2004 IEEE International Conference on Robotics and Automation, New Orleans, LA, USA, 2004, pp. 284–289. http://doi.org/10.1109/CACSD.2004.1393890.

[34] Mosek ApS, The MOSEK Optimization Toolbox for MATLAB Manual, Version 7.1 (Revision 63), https://docs.mosek.com/7.1/toolbox/index.html (Accessed 26 May 2018)